THE JOURNAL OF COMPARATIVE NEUROLOGY 343:370–386 (1994)

Are There Three Types of Horizontal Cell in the Human Retina?

HELGA KOLB, EDUARDO FERNANDEZ, JAMES SCHOUTEN, PETER AHNELT, KENNETH A. LINBERG, AND STEVEN K. FISHER

Ophthalmology Department, John A. Moran Eye Center, Salt Lake City, Utah 84132 (H.K., J.S.); Neuroscience Institute and Department of Histology, University of Alicante, 03080 Alicante, Spain (E.F.); Departments of General and Comparative Physiology, University of Vienna, A-1090 Vienna, Austria (P.A.); Neuroscience Research Institute, and Department of Biological Sciences, University of California Santa Barbara, Santa Barbara, California 93106 (K.A.L., S.K.F.)

ABSTRACT

Golgi-impregnated horizontal cells (HCs) as viewed in whole mount human retinas have been studied by light microscopic (LM) techniques. Impregnated HCs have been drawn by camera lucida and by the Eutectics neuron tracing method to provide quantitative data on dendritic tree sizes, dendritic tree shapes, and dendritic terminals for statistical treatment and cluster analysis. In addition, fractal analyses of HC dendritic branching patterns have been performed.

Three significantly different HCs can be classified on both subjective and objective morphological criteria in central and peripheral human retina. In the fovea all HCs are so small that it is difficult to achieve a clear separation of the subtypes, although they can be distinguished by the experienced observer. HI types are the classic HCs of Polyak (The Retina, Chicago: University of Chicago Press, 1941) with distinct dendritic terminal clusters going to cones and a fan-shaped axon terminal consisting of large numbers of rod-destined terminals. HII cells have profusely branched, overlapping dendrites, with poorly defined terminals going to cones and a short curled axon bearing small terminals also going to cones. The HIII types exhibit larger diameter, more asymmetrically shaped dendritic trees and 30% more dendritic terminal clusters than HI cells at any location on the retina. Many HIII cells appear to emit a process from the cell body in the inner nuclear layer (INL) that descends into the outer strata of the inner plexiform layer (IPL). The axon of the HIII cell may end in a loosely organized, sprawling arborization.

Fractal dimensions of the horizontal cells also show significant differences between the three groups. HII cells exhibit the highest fractal dimension followed by HI and HIII cells with lower and lowest fractal dimensions, respectively. The fractal dimension of HII cells of rhesus monkey, as determined from drawings by other authors in other publications, are the same as HII cells of human retina.

Key words: HI, HII, HIII, morphology, statistical analysis

Horizontal cells (HCs) are important interneurons of the first synaptic layer of the retina. Through lateral inhibition, feedback, and feed-forward interactions to photoreceptors and bipolar cells, they initiate spatial and spectral opponency for receptive field organization of second- and third-order retinal neurons (Werblin, 1969; Baylor et al., 1971; Kaneko, 1973; Dowling, 1987, for a review). In retinas of nonmammalian species in which there is good trichromatic or even tetrachromatic vision, three or four types of HC can be recognized morphologically and are known to have color-specific connections to cones (Stell and Lightfoot, 1975; Leeper, 1978; see Kolb and Lipetz, 1991, for a review). Physiologically, such "color-coded" HCs have been identified as "chromaticity units" (Svaetichin and MacNichol, 1958; Spekreijse and Norton, 1970; Fuortes and Simon, 1974).

In mammalian retinas, when the animals have dichromatic color vision, two types of HC have been described (Cajal, 1892; Boycott, 1974; Kolb, 1974; Wässle et al., 1978;

Accepted October 29, 1993.

Address reprint requests to Helga Kolb, Ophthalmology Department, John A. Moran Eye Center, University of Utah Health Sciences Center, 50 N. Medical Drive, Salt Lake City, UT 84132.

Mariani, 1985; Gallego, 1986). Neither type in these species appears to be selective for spectral cone types by morphological criteria alone, although some differences in wavelength sensitivity have been determined physiologically (Nelson et al., 1985, 1990). These two types of HC have been shown to provide surrounds for ganglion cells (Mangel, 1991).

Until recently, monkey and human retinas were also thought to have two types of HC, as in the rest of the mammals. The HI type is the one originally described by Polyak (1941), and it is known to contact cones at its dendrites and rods at its axon terminal (Boycott and Dowling, 1969; Kolb, 1970; Gallego, 1986; Linberg and Fisher, 1988). The second type, the HII cell, was distinguished as different from HI in 1980 (Kolb et al., 1980) and is now generally accepted as being a purely cone-connected HC (Boycott et al., 1987; Wässle et al., 1989; Wässle and Boycott, 1991; Kolb and Lipetz, 1991; Kolb et al., 1992). The two types of HC in primates have been suggested to be the equivalent of the A- and B-types, present in nonprimate mammals, both in showing similar overall photoreceptor connections and in supposedly having no spectral selectivity (Boycott et al., 1987; Wässle et al., 1989; Wässle and Boycott, 1991). Since rhesus monkeys and humans have good trichromatic color vision, one might expect the organization of their HCs to bear some similarity to those of other vertebrates with similar good color vision. Thus perhaps three types of HC, as occur in fish retinas, might be found. Moreover, one could also entertain a hypothesis that HCs in trichromatic primates might have spectrally specific connectivities to cone photoreceptors (Gouras and Zrenner, 1981).

In this paper, we demonstrate that three types of HC can be distinguished in the human retina on morphological criteria that can be described by both subjective and objective criteria. The third, HIII, type was added when some of the authors of this paper thought they were subdividing HI and HII cells into a data set for quantitative analysis of dendritic field sizes with eccentricity. Instead of HII types being discerned, the HI types had been subdivided into two subtypes. The new subtype, which we have called *HIII* (Linberg et al., 1987; Kolb et al., 1992), proved to be approximately 40% larger in dendritic field area, was often more asymmetrical, and bore 30% more dendritic terminal clusters, probably destined for cones, than neighboring HI cells at any point on the retina.

Following these initial reports (Linberg et al., 1987; Kolb et al., 1992), we have gone on to put the finding of a new HIII type on a more objective basis. Statistical analysis of over 600 HCs in several different Golgi-impregnated retinas has shown that HCs fall into three subtypes. In a further attempt to unbias the data of this paper, one of the authors, who was a totally naive observer, was set the task of drawing 110 impregnated HCs by the Eutectics neuron tracing system, and then we applied multivariate statistical and cluster analyses to this database. The findings further confirm that the HCs of the human retina fall into three distinct morphological types. Furthermore, a fractal analysis of dendritic trees of the three HC types confirms the morphological differences and provides an objective numerical value to this classification scheme (Fernandez et al., 1992b, 1994).

Evidence for these three subtypes being involved in different chromatic tasks based on their differences in connectivity to cone spectral subtypes is given in the accompanying LM and electron microscopic (EM) analyses (Ahnelt and Kolb, 1994a,b).

MATERIALS AND METHODS

Human eyes

Human eyes were obtained from several southern Californian eye banks (UCLA, Loma Linda, Lions Doheny, Orange County, and San Diego eye banks). All were corneal donor eyes free of retinal pathology and came from a mixture of age groups and sexes. The specimens were collected as part of a large-scale anatomical investigation of the human retina processed by Golgi techniques. The methods for fixation and Golgi impregnation are given in a previous publication (Kolb et al., 1992). We estimate shrinkage of human retina to be no more than 10% after these whole mount Golgi procedures. We have made no correction for shrinkage in the quantitative methods used below.

Methods of analysis

Zeiss MOP computer analysis of camera lucida drawings. Whole mounted human retinas were examined by LM and HCs from 12 different, well impregnated retinas were used for the analysis. All areas of retina were examined for HCs. Cells were drawn with a camera lucida on a Zeiss research microscope. It was important that all HCs were drawn in groups of cells that were impregnated in close vicinity to each other so that dendritic field sizes were always compared. The drawn HCs were then plotted on a map of the whole retina to place their location relative to the fovea. Distances were measured in millimeters of eccentricity from the center of the fovea. Six hundred fifty HCs were analyzed for dendritic tree area by entering data on the cross-sectional area of linearly connected end points of dendrites in a circular path, plus data on the number of dendritic terminal clusters, into a Zeiss MOP computer system. Statistical tests on these data were performed using the SPSS/PC+ Advanced Statistics Package (SPSS Inc.).

Eutectics neuron tracing system. One hundred twelve HCs were drawn on the Eutectics neuron tracing system so that quantitative aspects of the cells could be computed (Capowski, 1989). We used the following parameters determined by the system: 1) process length, 2) membrane surface area (μm^2), 3) total cell volume (volume of the dendrites in μm^3), 4) soma cross-sectional area (μm^2), 5) soma mean diameter, 6) soma form factor (this parameter represents a measure of roundness and ranges between 0 (flat) and 1 (circular), 7) spine density, 8) swelling density (number of swellings or varicosities/μm^2), 9) number of segments (a portion of the tree from branch point to branch point), 10) segment length, 11) branch order (at the first branch point the order increases to 2 and so on), 12) area of influence (this represents the cross-sectional area of a polygon drawn around the farthest dendrites of the whole dendritic tree), 13) dendritic tree diameter (mean diameter of the polygon above in μm), 14) perimeter of the polygon (μm), 15) dendritic form factor (defined as the ratio of the polygon area to the area of a circle having the same circumference), and 16) fractal dimension (see below). We also counted the number of dendritic terminal clusters on each cell in the case of HI and HIII cells. HII cells have a disorganized, profuse branching pattern, and their dendritic terminals are not clearly organized into dendritic terminal clusters and so are not easily quantitated for this feature.

Cluster analysis. To determine whether the HCs could be classified into several groups, we performed a cluster analysis. This analysis allows objects or cases to be classi-

fied into categories by searching for relatively homogeneous groups of features. Seven agglomerative clustering algorithms from the SPSS/PC+ Advanced Statistics software package were applied. The algorithm that produced the clearest cluster structure was the Ward's method.

Statistical validation. Statistical validation was performed as described in another paper (DeJuan et al., 1992). We used three procedures. 1) We made correlations between groups yielded by the different cluster methods by constructing contingency tables and measuring the degree of correlation by Cramer's V. 2) We assessed cluster consistency by obtaining randomly selected subsamples of the data and comparing these subsamples to the total sample cluster by contingency tables and Cramer's V. 3) We determined whether the groups produced by our analysis were discrete enough to be distinguished by applying discriminant analysis. Discriminant analysis is a multivariate statistical method that allows one to identify the variables that are important for distinguishing among groups or objects (horizontal cells in our case) and develop a procedure for predicting group membership for these objects and for new cases whose group membership is undetermined. We used the Jackknife validation procedure to reduce bias in group classifications (Klecka, 1980; Manly, 1986).

Fractal dimension. Fractal dimension (D) was calculated by the grid method described in greater detail elsewhere (Fernandez et al., 1992b, 1994) using the IMAGE software program (Rasband and Sheriff) available from the National Institutes of Health. Eutectics drawings and drawings of other authors were scanned into a Macintosh IIsi and analyzed by the fractal portion of the IMAGE program.

RESULTS

Morphological appearance of HCs in the human retina

Figures 1 and 2 show camera lucida drawings of HCs as they appear at different eccentricities in the human retina. The micrographs in Figure 3 illustrate HCs found close to each other at 10 mm eccentricity in one human retina. Although they are most obvious at eccentricities beyond 5 mm (Figs. 2, 3), three morphologically distinct types of HC can be discerned at all retinal locations. A distinction between HI and HII cells is clearest because of obvious differences in branching patterns. The distinction between HI and HIII has to be made on comparisons of two cells lying side by side, because the major difference between them is in the size of their dendritic trees.

The cells lying at 200 μm and 350 μm from the fovea (Fig. 1) are some of the closest examples to the foveal center that we found. Cells at 200 μm have a stretched appearance and are in fact larger in diameter than cells of the foveal slope, probably because they are reaching out to contact the widely spaced and scarce cone pedicles of this region (Ahnelt and Keri, 1991; Fig. 1, 200 μm). At 350 μm from the fovea, the HCs appear to be of two different dendritic tree sizes. Some of them are very small in dendritic tree diameter (15 μm across), possess an axon, and have bushy dendrites converging with many terminals upon what are probably four closely packed, small-diameter cone pedicles. These we identify as HI cells (Fig. 1 HI, 350 μm). The other two HCs in Figure 1 (350 μm) have much larger diameter dendritic trees (30 μm for the longest axis). The one that we think is an HII has a profusion of wispy dendrites and few clear terminals, while the other has lesser numbers but thicker dendrites and seven distinct terminal clusters. We suggest that the latter HC is an HIII type (Fig. 1, HIII, 350 μm). By 500 μm from the fovea (which is still on the foveal slope), three types of HC can be more easily recognized. HI cells have a compact, bushy dendritic tree, giving rise to large, round dendritic terminals clustered in a manner that suggests their contacting five closely packed cone pedicle bases. HII cells are now evident as the more "wooly looking" cell type, larger in dendritic tree diameter and with the ill-defined clusters of terminals making it difficult to say how many cones they might contact. HIII cells, in contrast, are heavyset cells with asymmetrical dendritic trees and dendrites bearing terminal clusters to fit seven to nine cones. In overall appearance, HIII cells resemble the HI cell but have larger dendritic fields (Fig. 1, *HIII*, 500 μm). At 2.5 mm eccentricity, the three different HC types can be distinguished on the criteria that were just becoming noticeable for cells on the foveal slope (Fig. 1, HI, HII, HIII, 2.5 mm). HI cells appear to contact seven cones, while HIII cells appear to contact 12 cones. HII cells have the typical disorganized, profuse branching pattern (Kolb et al., 1980; Boycott et al., 1987), and it is difficult to estimate how many cones they may contact.

Beyond the central 5 mm radius from the fovea and into peripheral retina, the three types of HC can be clearly distinguished (Figs. 2, 3). HI cells have the typical appearance described by Polyak (1941), with distinct radial dendrites ending in definite clusters of large, round terminals directed at overlying cone pedicles. HIII cells by comparison are much larger in field size and usually have a distinct asymmetry, with one or two longer, thick dendrites projecting out farther from the cell body than the remaining dendrites. More dendritic terminal clusters are evident than on HI cells, and moreover, numerous gaps in the regular array of clusters suggest that some cone pedicles that lie over or close to the major dendrites are being missed (Figs. 2, 3e; Ahnelt and Kolb, 1994a,b). HII cells are more obviously different from the other two types in being profusely branched and having many wispy, crisscrossing dendrites (Figs. 2, 3c). The dendritic tree diameters of HII and HI cells look comparable in the peripheral retina, but the tree size of HIII cells is always significantly larger than that of either of the other two (Figs. 2, 3e).

All three types of HC appear to have an axon. Type HII has a short, curled axon that arises from a dendrite and passes some 200–400 μm in a meandering manner away from the cell body (Figs. 2, 3d). Occasionally, the axon even comes back upon the cell body to mix with terminals of the dendrites. The single terminals or small clusters of two or three terminals, produced along the length of the axon, are known to innervate cone pedicles (Figs. 2, 3d; Kolb et al., 1980; Ahnelt and Kolb, 1994a,b). Axons belonging to HI cells are thick (1–2 μm diameter) and usually run rather straight out from the cell body or a primary dendrite (Fig. 2, arrow) for 300–500 μm before impregnation fails. Only a few examples of a complete HI cell, from cell body to axon terminal, in the rhesus monkey have ever been illustrated (Mariani, 1985; Rodieck, 1988) but those that have clearly show that the axon terminal is a fan-shaped, compact group of branches and terminals such as are illustrated in Figures 3b and 4A (HIAT). HIII cells also produce an axon from their cell body or a major dendrite, which, like that of the HI cell, runs off in a relatively straight trajectory (Figs. 2, 3e,

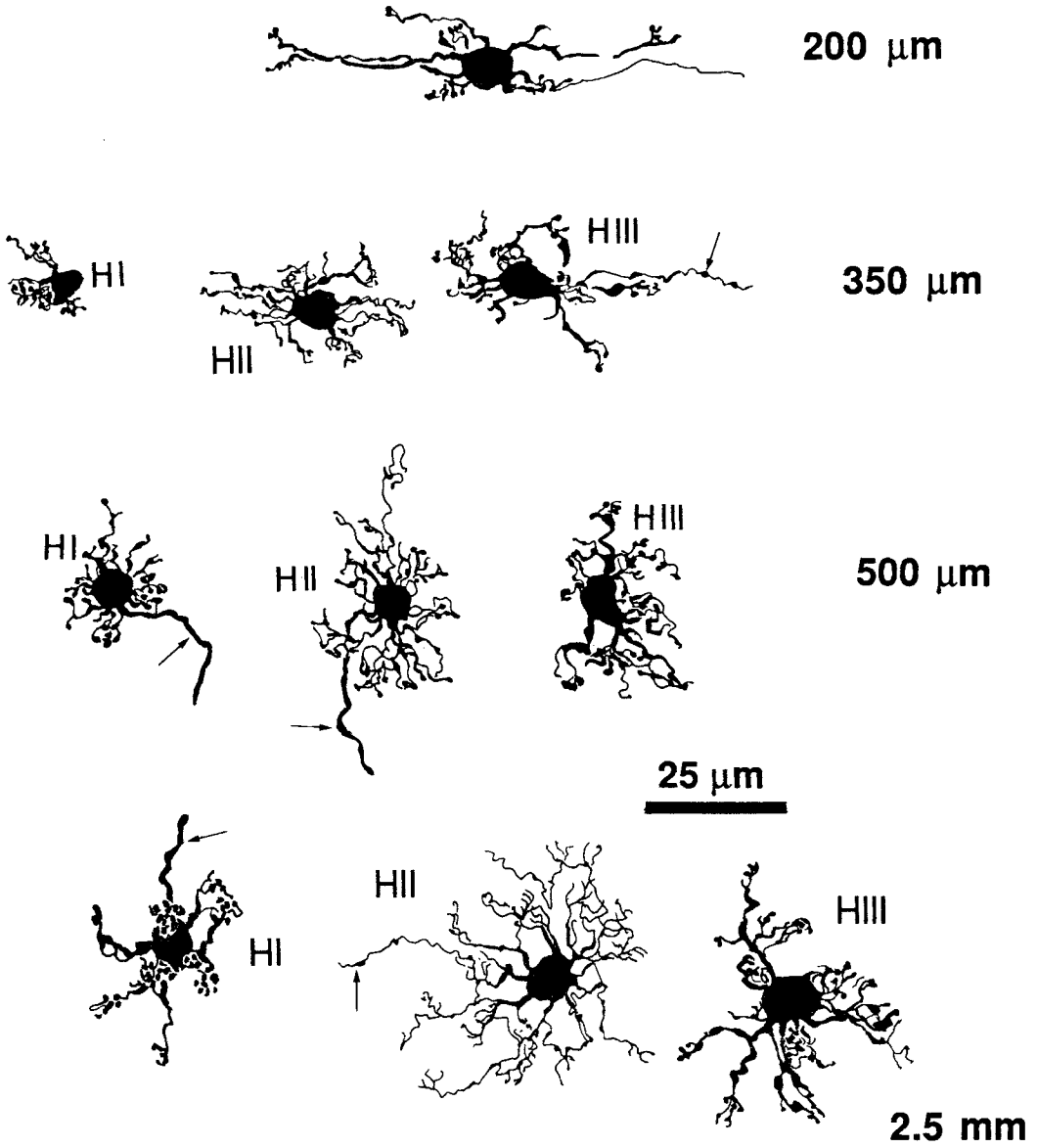

Fig. 1. Camera lucida drawings of horizontal cells (HCs) found in the fovea, foveal slope, and within the first 2.5 mm from the center of the fovea. In the fovea, HCs are elongated and stretched-looking (200 μm). On the foveal slope, the three types HI, HII, and HIII become recognizable, and by 2.5 mm the three types are more clearly classifiable. Axons are indicated by arrows.

arrows). The endings of HIII axons have not been seen in this study, but axon terminal arborizations that are more loosely organized and cover a greater area than the more compact HI axon terminals are commonly observed. We suggest that these might be the axon terminals of HIII cells (Figs. 3f, 4A, HIIIAT?).

Many HIII cells have descending processes to the IPL

During the course of our observations on HCs in the human retina, we noticed that many of the HIII cells emitted a process that descended through the INL into the outer strata of the IPL. All such "bistratified" HCs also had a normal axon that remained in the OPL. The descending processes of HIII cells were frequently quite similar to bipolar cell axons. They branched into one or two short secondaries that gave rise to fine, beaded processes that were narrowly stratified in the outer portion of the IPL or even partially in the amacrine cell layer of the INL. Figure 4B,C shows two examples from 8.5 mm and 15 mm eccentricity, respectively, where the descending process going to the IPL arose from the lower surface of the HIII cell body. Other variations on these bistratified HCs include the descending process coming from a large primary dendrite and running laterally for some distance in the OPL before turning down into the INL to reach the IPL or projecting laterally from the cell body in the INL before turning to plunge downward into the IPL. We have no systematic quantitation of how frequently these HIII cells with descending processes occur, but it was notable enough (we have drawn dozens of them) that we suggest that they

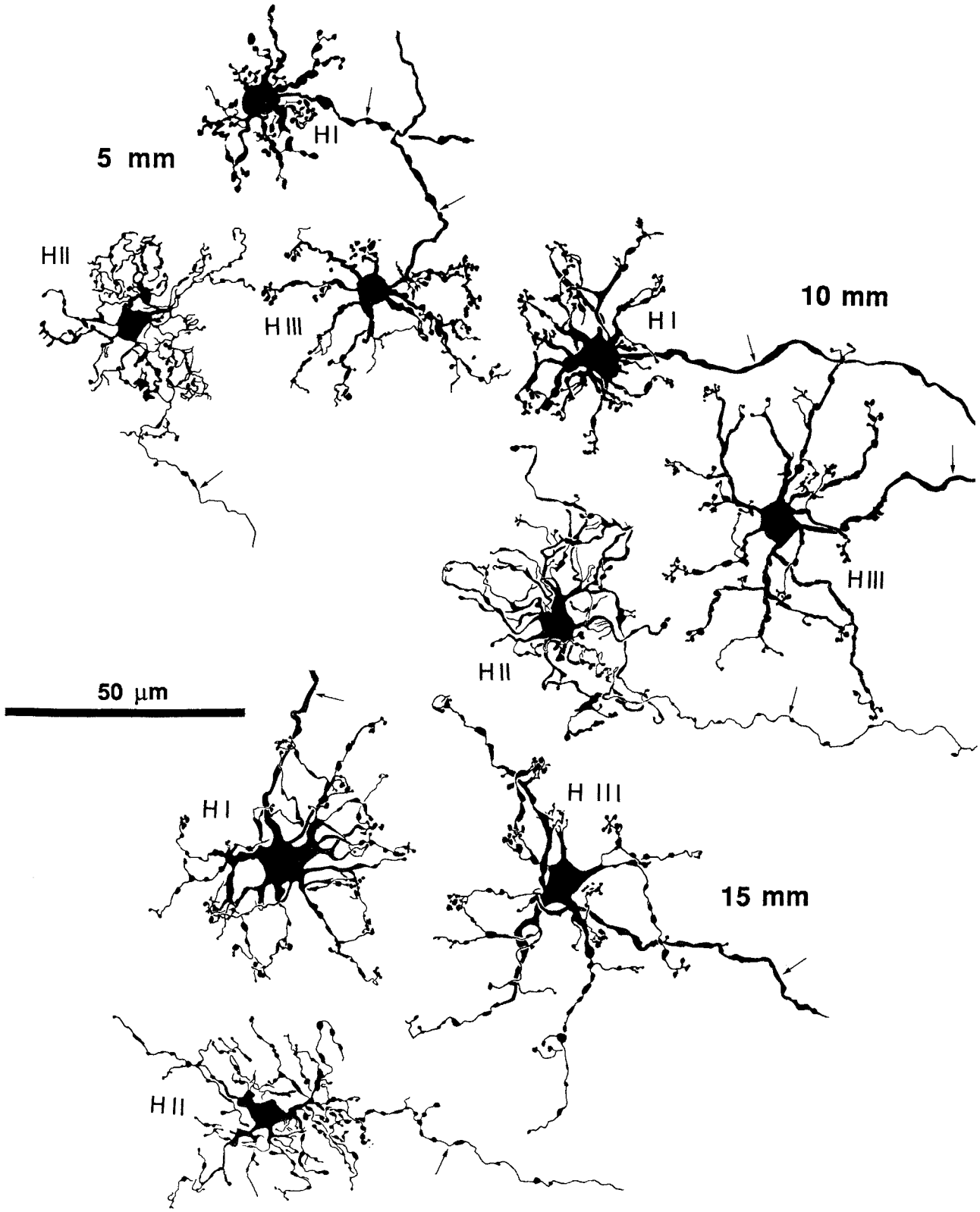

Fig. 2. The three HC types are distinguishable by morphological criteria at 5 mm, 10 mm, and 15 mm eccentricity from the fovea. All three types have axons indicated by the small arrows.

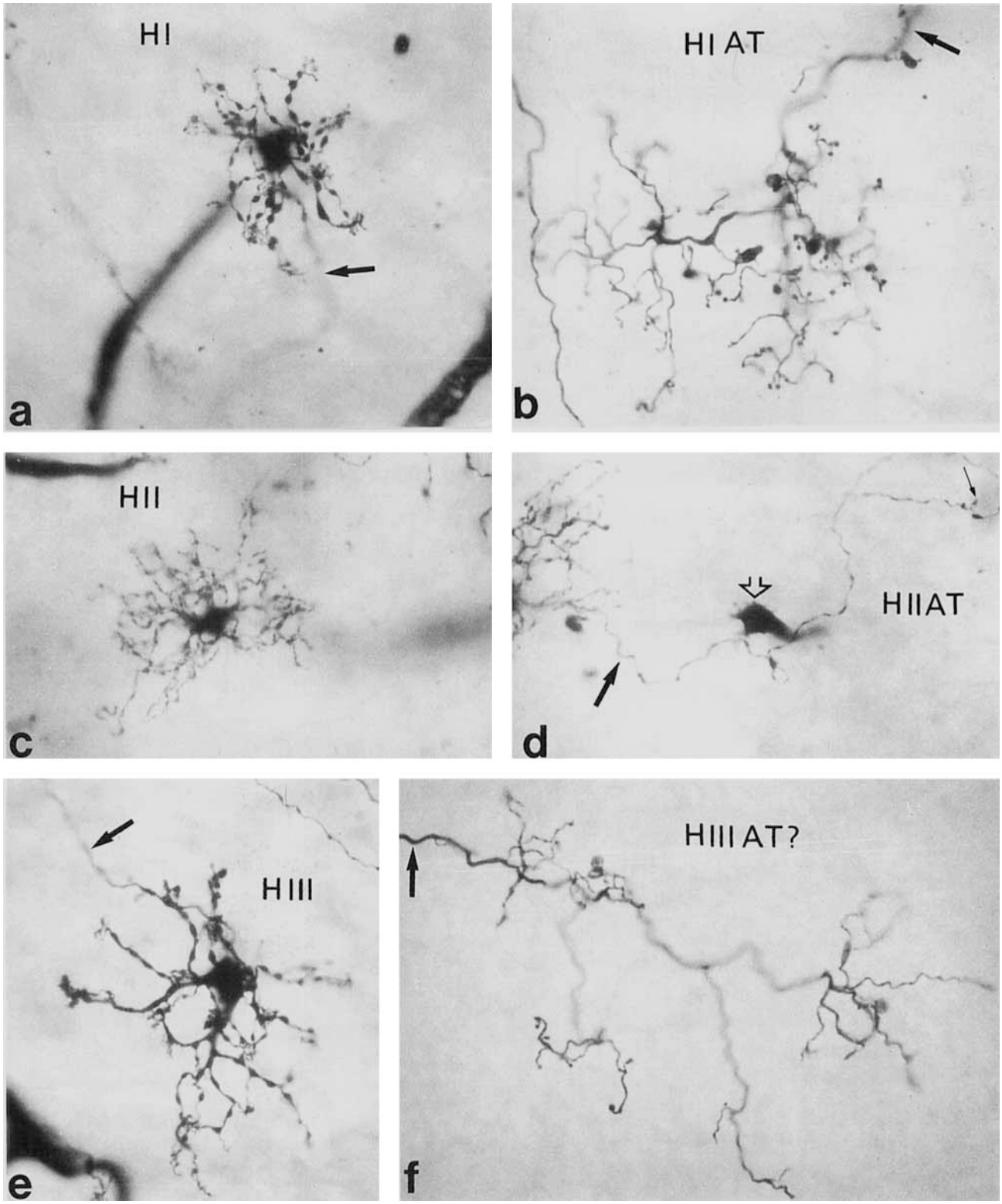

Fig. 3. Light micrographs (LMs) of the three types of HC taken from closely situated cells at 10 mm eccentricity in one human retina. **a:** HI type cell with a small compact dendritic field has distinct clusters of terminals contacting 13 cones. Axon is out of focus (arrow). **b:** HI type axon (arrow) expands into a fan-shaped terminal arborization containing many terminals known to innervate rods. **c:** HII cell has an irregular, wooly-appearance and ill-defined dendritic terminals. **d:** A curly, thin axon of an HII cell (large black arrow) runs a short distance and loops around upon itself. Only one small terminal is impregnated (solid arrow). A cone pedicle is Golgi-impregnated but apparently does not receive a terminal from the HII axon (open arrow). **e:** An HIII cell has a dendritic tree that is 40% larger than HI (a) and is asymmetrical in shape. The dendrites end in 23 distinct clusters of terminals. The axon is indicated by an arrow. **f:** A putative HIII axon (arrow) ends in a loose, sprawling arborization that bears few terminals. ×770.

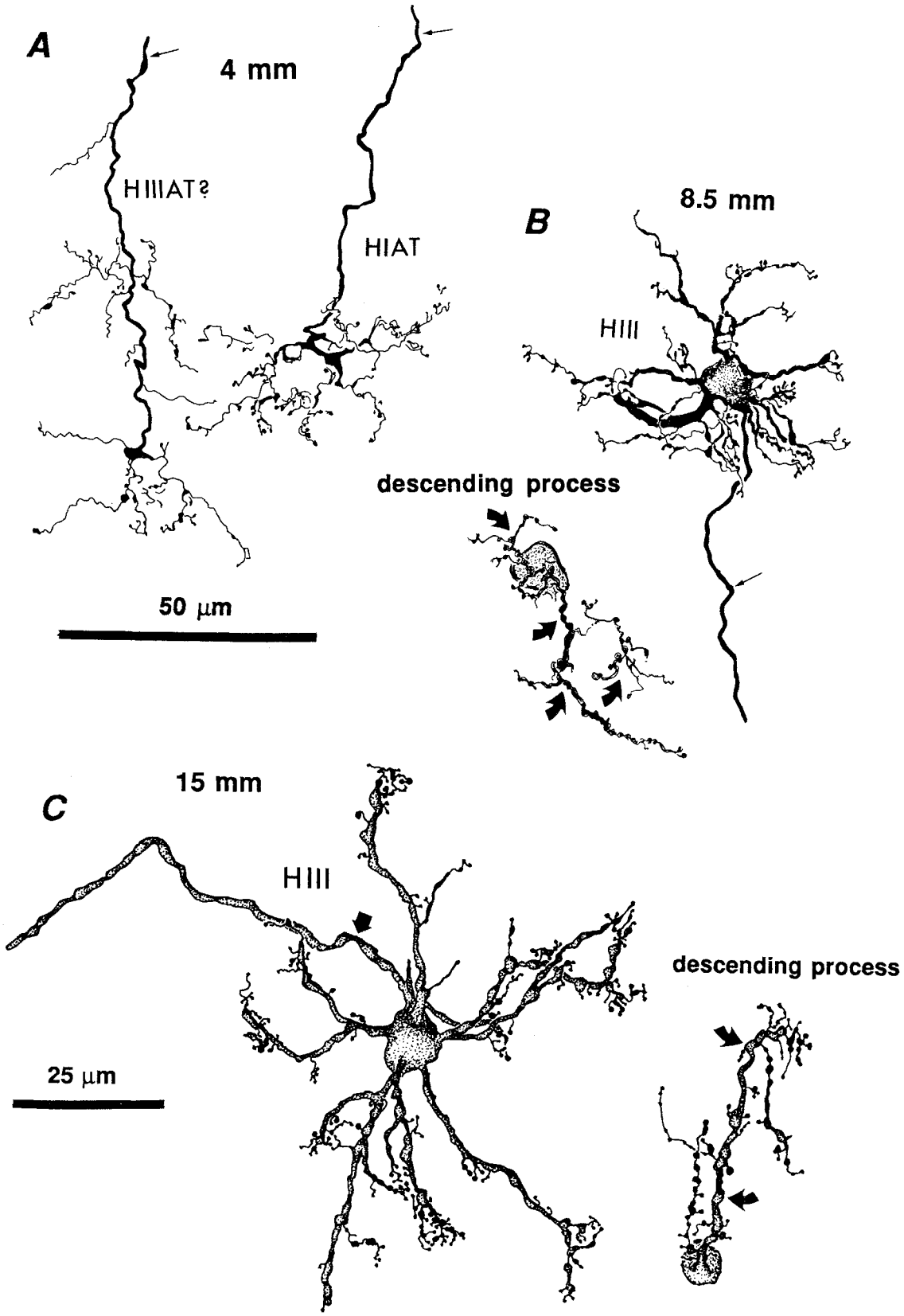

Fig. 4. **A:** Camera lucida drawings of HI (HIAT) and putative HIII axon terminals (HIIIAT?) found at 4 mm eccentricity. Straight arrows in A and B indicate axons. **B:** An HIII cell, found at 8.5 mm eccentricity, has a descending process to the inner plexiform layer (IPL) that branches in "bipolar axon terminal-like" fashion (curved arrows). **C:** HIII cell from 15 mm eccentricity with a descending process branching in the outer strata of the IPL (curved arrows). The regular axon in the outer plexiform layer (OPL) is indicated by a straight arrow.

may form as much as 20% of HIII cells of midperipheral (Fig. 4B) and peripheral (Fig. 4C) retina.

Fractal dimensions of HCs in the human retina

Mandelbrot's (1982) fractal geometry has recently been applied to analysis of neurons in the central nervous system. Fractal dimension can provide a quantitative measure of the complexity of the borders of a neuron (Smith et al., 1989; Morigiwa et al., 1991; Porter et al., 1991; Fernandez et al., 1992b, 1994) and how completely the branches of a neuron fill its dendritic field. The measure is called *fractal* because it is usually a fraction and not a whole number. It is called a *dimension* because it provides a measure of how completely an object fills space. For example, in two-dimensional space, a D value of 1 would represent a one-dimensional straight line, while a D value of 2 would represent a two-dimensional plane completely covering this area. Since nerve cells seen in two dimensions are not straight lines and they do not completely cover the two-dimensional area, their D values fall between 1 and 2. Neurons with lower D values have relatively few dendritic branches, while neurons with higher D values are more profusely branched and fill their dendritic fields more uniformly.

We have calculated D values of 112 HCs drawn by the Eutectics automated drawing system. The HCs were from five different human retinas and eccentricities ranging from 6 to 20 mm from the fovea. The HCs were entered into the computer by a naive observer who did not select cells for type but rather for their being isolated enough from neighboring cells and therefore easy to draw. Among the 112 cells, all but four were HI or HIII cells. Drawings of representative HI and HIII cells and their D values are illustrated in Figure 5. The four HII cells drawn on the Eutectics system (one of them illustrated in Fig. 5 and another in Fig. 6) were from 10 to 15 mm eccentricity. We do not have comparison of D values for Eutectics-drawn HII cells at other eccentricities, i.e., closer to the fovea or more peripherally in the retina, as we have for the other HC types (however, see later in Results, where we show that D values for HII cells from various eccentricities and from other authors' data. The HII cell in Figure 5 is quite representative of HII cells in general).

As can be seen, D values for HI cells are consistently higher than D values for the larger HIII cells at whatever eccentricity they occurred. Also, the D value for HII cells (Fig. 5, 11–13 mm) was much higher than that of either HI or HIII. When the D values of all 112 HCs are considered, it is clear that this type of measure differentiates the three groups (Table 1). An analysis of variance followed by a pair-wise test for differences between group means (Scheffe F test) shows the mean D values of each group, i.e., HI vs. HII, HI vs. HIII, and HII vs. HIII, to be significantly different ($P < 0.01$).

It is noticeable from the Eutectics-drawn cells (Fig. 5) that HI and HIII cells of central retina (6 mm) have higher D values than HI and HIII cells in peripheral retina. There appears to be an inverse relationship between fractal dimension and greater eccentricity from the fovea. Undoubtedly this is due to the facts that HCs are designed to innervate cones and that, with eccentricity from the fovea, the cones become more and more widely spaced, meaning that the HCs have to stretch their dendrites farther and farther; i.e., their dendritic tree area increases with eccentricity. Evidently the cells also become less bushy as cones become more widely spaced, leading to lower D values for both HI and HIII cells with eccentricity (Fig. 5).

TABLE 1. Mean and Standard Error of the Fractal Dimension (D) in 112 Human Horizontal Cells

Horizontal cell type	D value	SE	Number
HI	1.51	0.010	69
HII	1.61	0.010	4
HIII	1.47	0.011	39

In contrast, the HII cells, with inherently higher D values to begin with, do not seem to exhibit the same centroperipheral decline in D value. We wanted to see whether this was a generalized finding in other Golgi preparations and other primate retinas. In Figure 6 we illustrate several HII cells from different eccentricities and species drawn by different persons utilizing different drawing methods. All the cells, even those from the rhesus monkey, have comparable D values. Moreover, D values for cells from central retina vary over the range 1.57 (monkey HII cell A from Kolb et al., 1980) to 1.62 (monkey H2 cells C and D, from Boycott et al., 1987; Wässle et al., 1989), as do cells from peripheral retina. Thus HII cell B and HII cells E and F from this study of the human retina (Fig. 6) have the exact same range of values. It appears that HII cells in human and monkey retinas do not differ significantly across species or within a species' retina with eccentricity (mean D = 1.59, SE 0.001).

Cluster analysis of HCs in human retina

In order to determine objectively whether the HCs of the human retina can be classified into groups, we turned to cluster analysis (see Materials and Methods). This statistical method is designed to solve the following problem: Given a sample of n objects, each of which has a score on P variables, devise a scheme for grouping the objects into classes so that "similar" ones are in the same class (Kachigan, 1982; Manly, 1986). The method is completely numerical, and the number of classes is not previously known. Thus we used it on the data generated from 45 Eutectics-drawn HCs that were from the same retinal location (14 mm from the fovea) and for which we had the parameters listed in Materials and Methods. In addition, we added the D value that we had acquired independently on the same cells.

Figure 7 shows a dendrogram of the hierarchical clustering analysis generated by the SPSS/PC+ program. The 45 HCs at the bottom are merged into clusters at different stages depending on their degree of similarity (or distance between clusters calculated within m-dimensional space, where m = number of parameters). The dendrogram (Fig. 7) points out the existence of three groups of HCs in this data set. We did not know the real composition of each group, only that cells 1–14 belonged to the first group, cells 15–41 to the second, and cells 42–45 to the third group. Later, by subjective evaluation, we determined that the three groups corresponded to HIII, HI, and HII cells, respectively (Fig. 7).

Discriminant analysis

To investigate the relative importance of the parameters used to classify the HCs (listed in Materials and Methods), we used a discriminant analysis as described elsewhere (DeJuan et al., 1992) and in Materials and Methods. By this

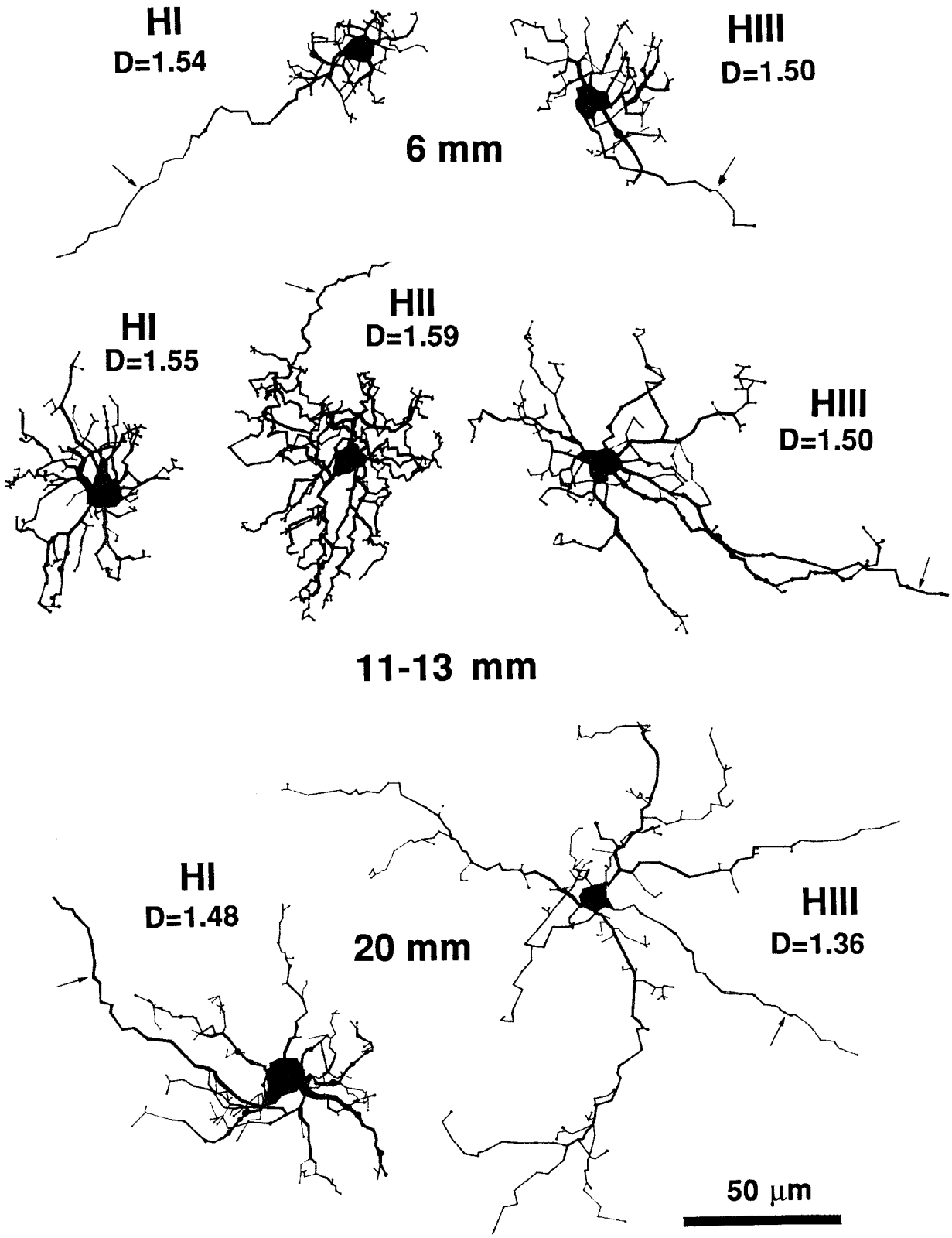

Fig. 5. Eutectics-drawn HCs at different eccentricities from the fovea to show their morphological differences and their individual fractal dimensions (D values). HI and HIII cells are shown at three different eccentricities. A single example of an HII cell is illustrated at 11 mm.

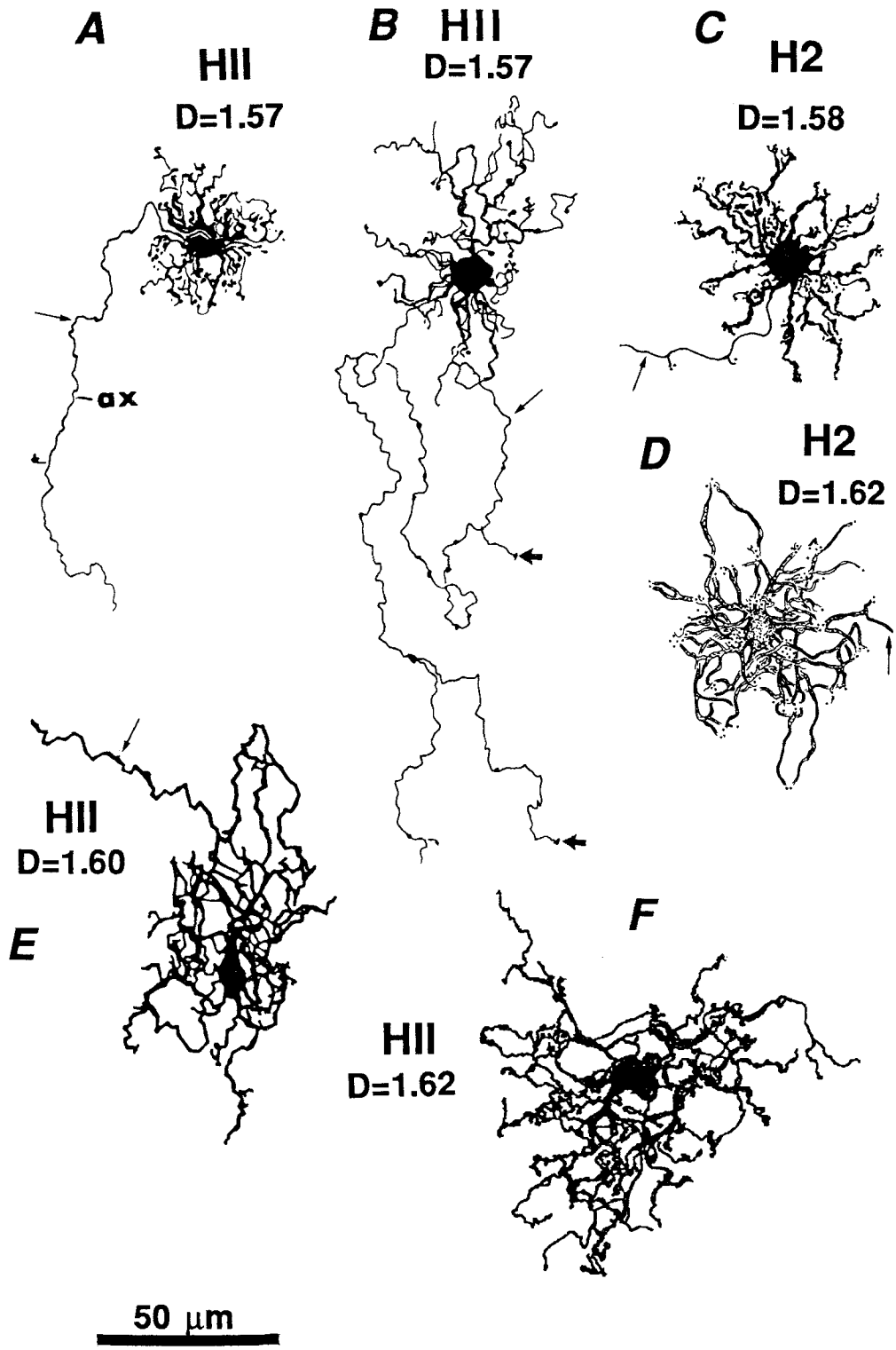

Fig. 6. Camera lucida drawings (A–D) and Eutectics drawings (E,F) of HII cells in different retinas and drawn by different persons. The D value of each cell is indicated. **A:** HII cell in rhesus monkey at 2 mm eccentricity (illustrated in Kolb et al., 1980). **B:** HII cell from human retina at 15 mm eccentricity. Some terminals on the axon are indicated at the thick arrows. **C:** An H2 cell in rhesus monkey at 4.3 mm eccentricity (reproduced by permission from Boycott et al., 1987). **D:** H2 cell from rhesus monkey at 5.7 mm eccentricity (reproduced by permission from Wässle et al., 1989). **E:** HII cell in human retina at 11 mm eccentricity. **F:** HII cell from human retina at 15 mm eccentricity. The axons (ax) are marked in all cases with a small arrow.

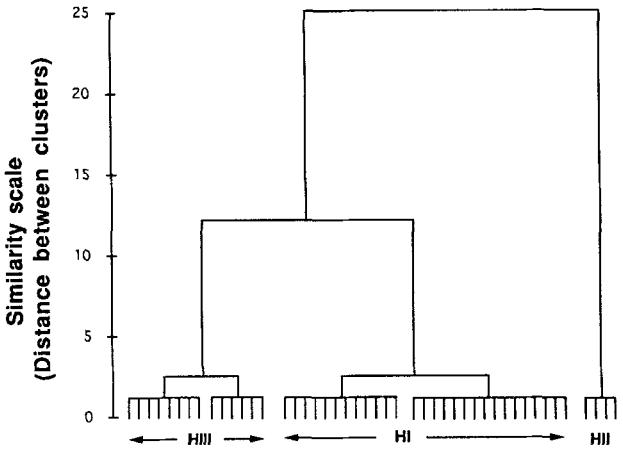

Fig. 7. A dendrogram of the cluster analysis (generated by the cluster module of the SPSS/PC+ Advanced Statistics) suggests that three groups of cells are present in a sample of 45 cells at 10–15 mm eccentricity. Data taken from Eutectics drawings from several human retinas.

analysis, the parameter with the highest power to discriminate between the different HC types is selected, followed by the parameter with the next highest discriminating power, and so on, until all the parameters are evaluated. Table 2 presents the six most useful parameters (steps) entered in each step of the discriminant analysis in order of significance. The first step, i.e., dendritic tree diameter, is the most significant parameter for discrimination between HI and HIII cells. The first through third steps are probably the most important for distinguishing HI and HII combined from HIII cells. Step four is probably important for discriminating HII cells from HI and HIII combined, thus forming the three groups seen in the cluster dendrogram (Fig. 7).

Based on the best discriminating combination of parameters, a classification matrix is produced by the program where each HC is classified into a group (HC type). The percentage of cases correctly classified is taken as an index of the effectiveness of the discriminant function. After we obtain an estimate of the misclassification rate using the "Jackknife" procedure (see Materials and Methods), the least biased group classification of the HCs is made, and the result is shown in Table 3. The overall accuracy of correctly classifying HCs in this manner was 96%. In particular, 100% of the HII cells were thus classifiable. Ninety-six percent of the HI cells were classified as HI (the other 4% were classified as HIII cells), and 94% of the cells were classified as HIII cells (the other 6% were classified as HI cells).

Although we used the full range of parameters available in the database, the analysis automatically rejected the number of dendritic terminal clusters from the analysis, because these are difficult to count on HII cells. However, using a discriminant analysis on only HI and HIII cells, the two most useful parameters were the number of dendritic terminal clusters and dendritic tree diameter. Thus, using only the dendritic tree diameter and number of dendritic terminal clusters, we were able to classify correctly a cell as HI or HIII 90% of the time.

Table 4 lists the mean and standard errors of the different parameters used in classifying the HCs, summarizing the data for these 45 HCs. It includes the D values. The Student's t test compares the HI and HIII cells for the various parameters and in the last column indicates which of these prove to be most significant (Table 4).

TABLE 2. *Stepwise Analysis: Steps in Order of Significance of the Variables To Discriminate Between the Three HC Types*

Step	Variable	Wilk's Lambda	Equivalent F
1	Dendritic tree diameter	0.448	25.81
2	Process length	0.198	25.56
3	Cell volume	0.137	22.62
4	Membrane surface	0.116	18.77
5	Segment length	0.109	15.37
6	Swelling density	0.102	13.11

TABLE 3. Predicted Group Membership (%) Using the Discriminant Analysis[1]

	Cell type		
Cell type	HI	HII	HIII
HI	96	0	4
HII	0	100	0
HIII	6	0	94

[1]The percentage of all cases correctly classified is 96%.

Quantitative analysis on HC dendritic field sizes and numbers of terminal clusters

We knew from previous studies that, like all retinal neurons, HI cells increase in dendritic tree size with greater and greater distances from the fovea (Kolb et al., 1980; Boycott et al., 1987). Since we had data from the cluster and discrimant analysis that HIII cells could be separated out as different from HI cells, we wanted to see whether HIII cells and HI cells independently increased in size in relationship to eccentricity in the retina. Six hundred fifty HCs in 12 different human retinas were subjectively identified as to being HI or HIII and were analyzed for dendritic field area calculated as star polygon areas (the linearly connected end points of dendrites in a circular path) and for numbers of dendritic terminal clusters (see below). This was a data set different from those for the 45 cells used for the cluster and discriminant analysis. The 45 cells of the latter data sets are plotted on the graphs of Figure 9A,B, so that their occurrence among the larger data set can be appreciated.

The dendritic field area (in μm^2) for 369 HIs and 210 HIIIs is plotted against eccentricity of the cells from the fovea in Figure 8A. In the first 5 mm from the fovea, the two types of HC have approximately the same dendritic tree areas and are not separable into size types on this kind of a graph but beyond 5–6 mm from the fovea HIII become separable from HI on dendritic area, occupying as a group the larger dendritic field areas (open symbols, Fig. 8A). A single, linear regression line can be fit to the data of the graph, but it provides a much weaker coefficient of determination. i.e., $r^2 = 0.39$, $P < 0.02$, than fitting two regression lines each with a significant coefficient of determination, i.e., for the HI cells $r^2 = 0.65$, $P < 0.0001$ and for the HIII cells $r^2 = 0.69$, $P < 0.0001$ (Fig. 8A, solid line and dashed line, respectively). This means that, pooling HI and HIII cells, only 39% of the variation in dendritic tree area is explained by differences in eccentricity from the fovea. On the other hand, 65% of subjectively named HI cells and 69% of subjectively named HIII cells have dendritic field areas that are accounted for by variation in eccentricity, when two regression lines are calculated. We also did an analysis of covariance using the dendritic tree area, the eccentricity

TABLE 4. Mean and Standard Error of the Different Variables for Each Horizontal Cell Type

Variable	HI (n = 27)	HII (n = 4)	HIII (n = 14)	HI–HIII (t test)
Process length	763.2 ± 36.5	1,238.9 ± 58.8	919.7 ± 67.4	$P < 0.030$
Membrane surface	1,459.0 ± 114.6	1,845.8 ± 209.9	1,472.1 ± 85.9	NS
Cell volume	323.3 ± 29.9	294.0 ± 55.4	280.2 ± 22.3	NS
Soma area	87.2 ± 3.1	81.2 ± 8.2	91.3 ± 4.0	NS
Soma diameter	10.5 ± 0.1	10.1 ± 0.5	10. 7 ± 0.2	NS
Soma form factor	0.69 ± 0.02	0.70 ± 0.05	0.76 ± 0.02	$P < 0.050$
Spine density	0.029 ± 0.006	0.021 ± 0.009	0.015 ± 0.003	$P < 0.050$
Swelling density	0.140 ± 0.008	0.110 ± 0.007	0.107 ± 0.004	$P < 0.001$
No. of segments	199.0 ± 15.9	233. 7 ± 18.0	139.0 ± 10.3	$P < 0.003$
Segment length	4.35 ± 0.33	5.35 ± 0.19	6.42 ± 0.24	$P < 0.001$
Branch order	12.3 ± 0.5	11.2 ± 0.7	12.2 ± 0.8	NS
Area of influence	3,733.9 ± 525.0	4,029.6 ± 474.7	7,037.2 ± 592.2	$P < 0.001$
Perimeter	226.6 ± 17.9	247.5 ± 8.5	326.7 ± 13.4	$P < 0.001$
Dendritic tree diameter	66.9 ± 3.9	71.2 ± 4.0	93.8 ± 3.8	$P < 0.001$
Dendr. form factor	0.81 ± 0.01	0.82 ± 0.04	0.81 ± 0.01	NS
Fractal dimension	1.53 ± 0.01	1.61 ± 0.01	1.47 ± 0.01	$P < 0.003$

from the fovea, and the cell type (named subjectively) as dependable variables. The analysis (performed using the MANOVA module on the SPSS/PC+ Advanced Statistics; see Materials and Methods) indicated that our data could be better described using two regression equations, one for HI cells and the other for HIII cells ($P < 0.001$). In addition, we tried different nonlinear functions (quadratic, logarithmic, exponential), but we did not see a greater significance ($P > 0.02$) than with the linear model. There is a significant difference ($P < 0.0001$) between the linear regression lines that were generated for HI and HIII cells (Fig. 8A).

A similar difference between HII and HIII cells is seen from 5 mm eccentricity into peripheral retina (Fig. 8B) based on an analysis of 281 cells (210 HIIIs and 71 HIIs). Again, the HII cells could be fit with a regression line and coefficient that an analysis for covariance indicated as significantly different from the HIII regression line and coefficient ($P < 0.0001$). Thus HIII cells at any point on the retina beyond 5 mm from the fovea are significantly larger in dendritic tree area than either HI or HII cells. The HI and HII cell groups overlap in dendritic tree size at all eccentricities, as can be seen in Figure 8C. The difference between regression lines fit to their distributions (Fig. 8C, solid and dashed lines, respectively) is not significant.

The difference between dendritic field areas for HI and HIII cells at different eccentricities in a single human retina is illustrated in another way in Figure 9. Here, the scatter in the data is appreciable, because we are lumping cell measurements within a 4–6 mm bin at the different eccentricities. From 0–6 mm, HI and HIII cells have overlapping dendritic field sizes, and lumping the data in this area where field size changes are rather small blurs the distinction between them. However, two cell groups can be assigned to different dendritic field size bins at eccentricities beyond 6 mm from the foveal center (Figs. 9B,C). Table 5 lists the averaged mean dendritic field areas of HI and HIII cells with eccentricity; here it can be seen that there is a difference between HI and HIII cells even within the first 6 mm of eccentricity, although there is a great deal of scatter in the data (large SEs). This is probably because the distinction between HI and HIII cells can really be made only by comparing two cells side by side, which may not always have be possible: Some misidentifications in this subjective evaluation are bound to have occurred.

Figure 10 shows a plot of the numbers of dendritic terminal clusters borne on the dendrites of HI and HIII cells as related to position in the retina from the foveal center. Dendritic terminal clusters were quantified on drawings of HCs by circumscribing clusters of terminals contained within the size of a putative cone pedicle projected from overlying cone inner segment mosaics (as was done originally by Boycott and Kolb, 1973, and demonstrated in the accompanying paper by Ahnelt and Kolb, 1994a). The plot (Fig. 10) indicates that HI cells have smaller numbers of terminal clusters than HIII cells at all eccentricities. The range for HI cells is from four clusters in the foveal area to 18 in far peripheral retina (Fig. 10). HIII cells, on the other hand, have a range from eight to 28 dendritic terminal clusters from fovea to 16 mm, respectively (Fig. 10). Table 6 summarizes these data. Again, an analysis of covariance, with accounting for the eccentricity effect, indicates a significant difference between HI and HIII cells ($P < 0.001$). Thus, as we saw in the discriminant analysis, the number of dendritic terminal clusters on HI and HIII cells serves also to distinguish between the two cell types.

DISCUSSION

In this LM study of Golgi-impregnated human retina, we have obtained morphometric and statistical evidence from an analysis of over 600 HCs that they fall into three distinct morphological types. The HC type originally described by Polyak (1941) can be subdivided into types HI and HIII on criteria of dendritic tree size, length of dendrites, numbers of contacts with cones, and fractal dimensions. The HII type, which was added to Polyak's groups a decade ago (Kolb et al., 1980; Boycott et al., 1987), is the third unique type of HC in the primate retina and was separated out from the HI and HIII types primarily on fractal dimension in the present study. This might be expected because of its more profuse and tufted branching pattern than either of the other two types (Kolb et al., 1980). The three types of HC are distinguishable not only on morphology and morphometry but also on connectivity with spectral cone types, a topic dealt with in detail in the accompanying papers (Ahnelt and Kolb, 1994a,b). We suggest that the answer to the question posed by the title of this paper is yes.

Morphological differences between HI and HIII cells

The difference between HI and HIII HCs was evident only after a great deal of observation and making a large number of drawings with both camera lucida and Eutectics computer-aided technologies. When examining the draw-

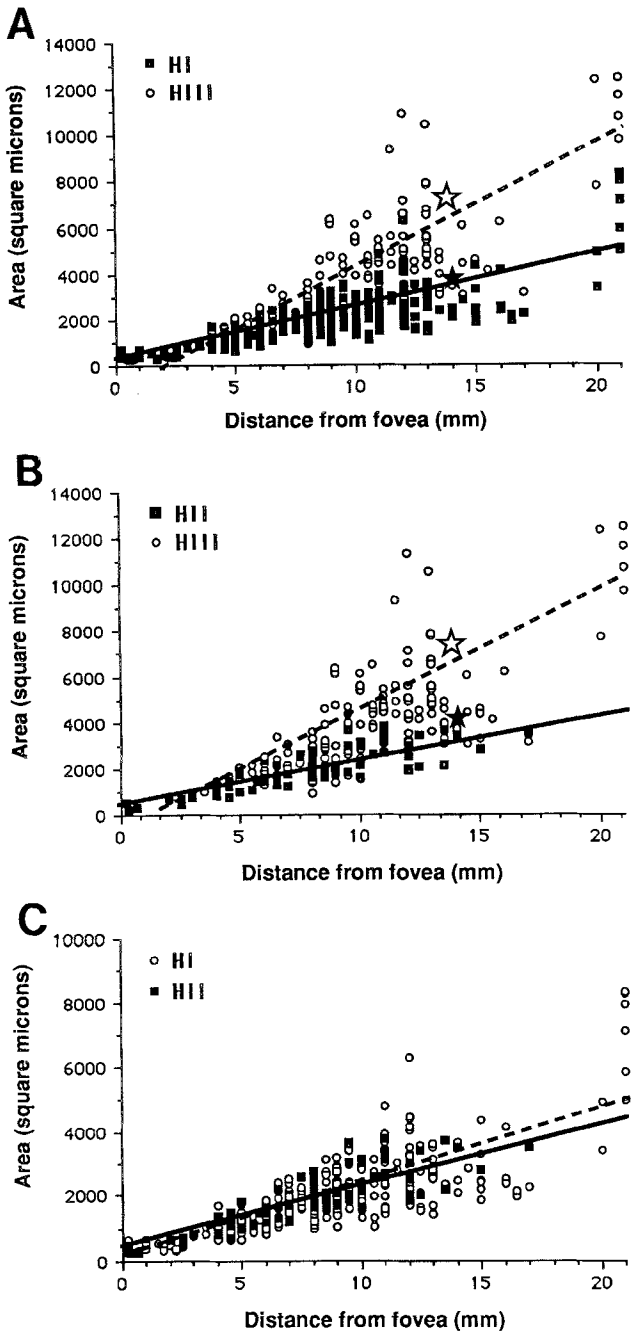

Fig. 8. **A:** Graph showing dendritic field area for HI and HIII cells plotted against eccentricity from the fovea. Data are pooled from several retinas (n = 579). Open star shows the mean size for 14 HIII cells from the cluster analysis (mean = 7,090 μm^2, SE 1,373). Solid star shows the mean size for 27 HI cells from the cluster analysis (mean = 3596 μm^2, SE 535). **B:** Graph showing dendritic field area for HII and HIII cells with eccentricity from the fovea (n = 281). Open star as for A. Solid star shows the mean size for four HII cells from the cluster analysis (mean = 4,028 μm^2, SE 560). **C:** Graph showing dendritic field areas for HII and HI cells with eccentricity from the fovea (n = 440).

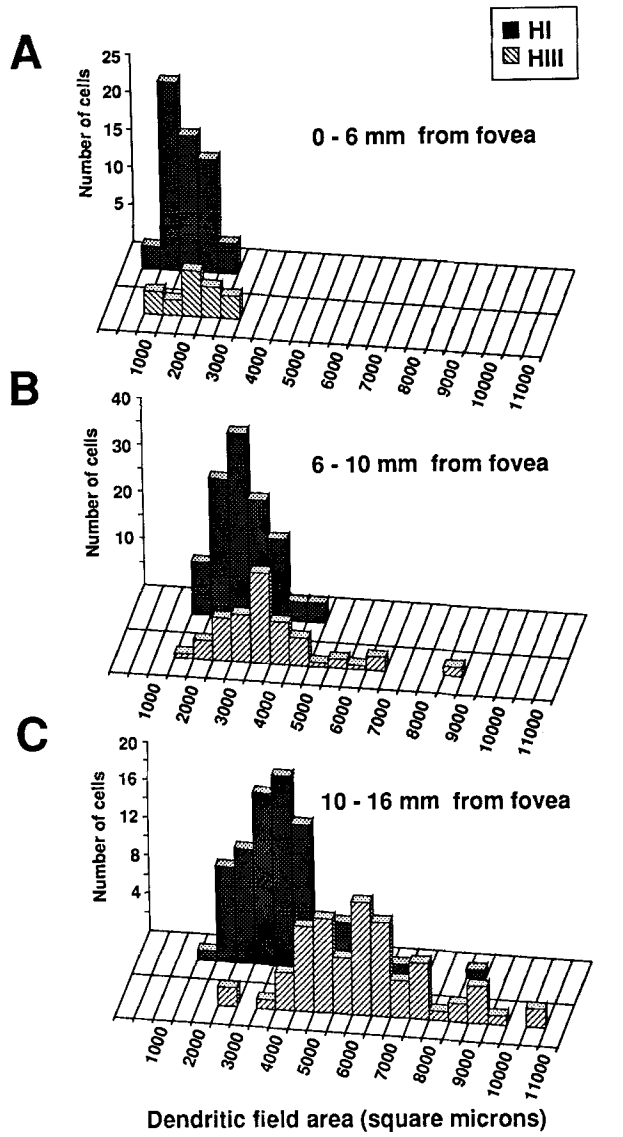

Fig. 9. Three-dimensional plots of dendritic field areas of HI and HIII cells at three different locations in the retina. **A:** 0–6 mm from fovea. **B:** 6–10 mm from fovea. **C:** 10–16 mm from fovea. The counts are from one human retina.

TABLE 5. Area of HC Dendritic Fields With Eccentricity in the Retina (in μm^2)

Eccentricity (mm)	HI (mean ± SE)	HIII (mean ± SE)
2–4	769.1 ± 78.0	1,037.8 ± 143.7
4–6	1,413.3 ± 66.4	2,129.6 ± 108.6
6–8	2,139.9 ± 74.6	2,834.1 ± 132.9
8–10	2,656.9 ± 82.1	3,699.8 ± 225.5
10–12	3,155.6 ± 147.1	5,928.0 ± 481.5
12–14	3,643.8 ± 221.4	6,591.3 ± 431.2
14–16	3,599.3 ± 325.2	6,100.5 ± 384.4

ings, which were originally part of a database on sizes of dendritic trees of HI and HII cells with eccentricity from the foveal center to compare with rhesus monkey data (Kolb et al., 1980), two size groups with parallel increases in dendritic tree diameters and significantly different regression lines fit to the data emerged (Fig. 8A). On looking at the drawings of the two cell groups, it was clear that the larger group did not consist of HIIs but instead consisted of cells that were a larger version of the standard HI cells.

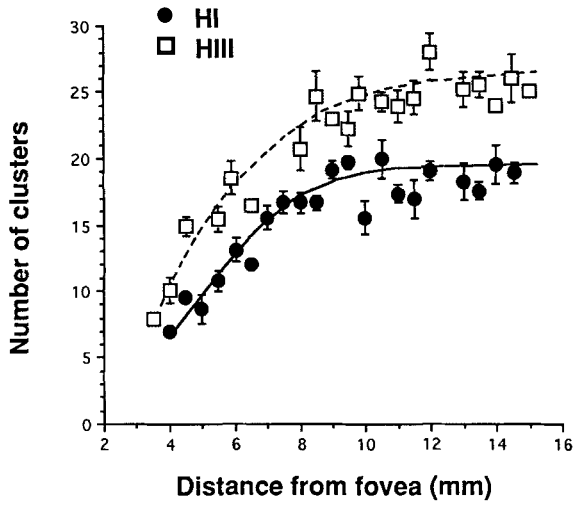

Fig. 10. Graph of the number of dendritic terminal clusters going to cones on the dendrites of HI and HIII cells. The counts were made on the same HCs as shown in Figure 8A.

TABLE 6. Number of Dendritic Terminal Clusters on HI and HIII Cells

Eccentricity (mm)	HI (mean ± SE)	HIII (mean ± SE)
2–4	6.0 ± 0.8	8.0
4–6	10.7 ± 0.4	13.4 ± 1.2
6–8	13.6 ± 0.3	17.5 ± 0.6
8–10	17.5 ± 0.3	22.7 ± 0.8
10–12	17.9 ± 0.5	24.6 ± 0.4
12–14	18.5 ± 0.6	25.6 ± 0.8
14–16	18.0 ± 1.4	25.7 ± 1.4

Large, asymmetrical, Polyak-type HCs were described for years as being the extremes of size for HI cells in far peripheral retina. Polyak (1941), Boycott and Kolb (1973), and Wässle et al., (1989) have all described such cells as HI types. We would now call these HIII types and, as we have seen from the data presented here, they occur alongside their smaller companion HI cells at all points in the retina. They are not simply phenomena of far peripheral retina. The relatively narrower size differential between HI and HIII dendritic trees and the asymmetrical aspect of the HIII morphology is not always obvious in central and near peripheral retina, particularly if impregnated HI and HIII cells do not lie side by side for size and shape comparisons. That is the reason why HIII cells have not been identified as a separate group before.

It could be argued that, in the survey of HCs done subjectively to pick cells as HI and HII for dendritic tree size comparisons with eccentricity, we were selecting cells specifically to fall into two size ranges, thus biasing the database and arbitrarily defining a new HIII type. To counter this criticism, we commissioned a naive observer who could not distinguish the HC types to draw about 100 HCs with the Eutectics neuron-tracing system. From this computer database, we could perform a cluster analysis on 45 of the HCs found in approximately the same area of retina. Using the quantitative parameters available from the Eutectics-drawn HCs, they became split into three groups by the cluster analysis (Fig. 7). The morphometric parameters that distinguished the members of the three groups could be objectively measured, rated by the computer, and a discriminant analysis applied. Thus, with no one among the authors choosing cells to place into the HI, HII, and HIII classification, the computer independently places the cells into three different groups at the 96% level each for cells we would call HIs and HIIIs and at the 100% level for cells we would classify as HIIs (Table 3).

The HIII cells with their larger dendritic trees and far-reaching dendrites could obviously contact more cone pedicles than the smaller HI cells. In fact, the quantitative data on dendritic terminal clusters (Fig. 10) reveal that HIII cells contact about 30% more cones at any point on the retina than HI cells. HIII cells close to the fovea contact 8–12 cones, and by the far peripheral retina they contact as many as 25–35 cones. In contrast, HI cells connect with 4–5 cones in fovea and 15–20 cones in the farthest periphery. An interesting relationship emerges between the dendritic field area of the HI and HIII types and the cone photoreceptor density innervating them (Fig. 11A,B). Thus, if the dendritic field areas of HI cells at different eccentricities listed in Table 5 are compared with the number of possible cones in such fields (Curcio et al., 1990), then HI cells have a 90% coincidence of dendritic cluster number with possible number of cones within the area covered by their dendrites (Fig. 11A). Even though HIII cells have approximately 40% larger dendritic fields, there is only about a 70% coincidence of their terminal clusters with overlying cones (Fig. 11B). This suggests that HIII cells are systematically related to fewer cone types across the retina.

We show elsewhere that HIII cells avoid contact with blue cone pedicles (B-cones; Ahnelt and Kolb, 1994a,b). It is probable that the 10% B-cone population as well as some of the G- and R-cones constitute the missed 30% of cones in HIII cell dendritic fields. Furthermore, it is possible that the asymmetrical dendritic trees characteristic of HIII cells are the consequence of their avoidance of B-cones in their fields.

In addition to differing in dendritic field size, shape, and number of cones contacted, HI and HIII cells may differ in the morphology of their axon terminals. The fan-shaped terminal arborization, with a high density of terminals destined for rod spherules, is well established as belonging to the HI type in rhesus monkey retina (Polyak, 1941; Boycott and Dowling, 1969; Kolb, 1970; Mariani, 1985; Rodieck, 1988). However, it is interesting to note that Boycott and Dowling (1969) originally pointed out two forms of HC axon terminals. One of the types was more loose and sprawling in morphology than the other, giving the impression to the authors of perhaps contacting cones as well as rods. We believe that these axon terminals may be associated with HIII cells. However, further studies to stain complete HIII cells and to ascertain whether their axonal connectivity differs from that of HI axon terminals will have to be carried out.

HIII cells with processes in the IPL

A large subpopulation of HIII cells appear to have a process coming off the cell body or a primary dendrite that descends into the INL and IPL, there to end as a varicose, narrowly stratified, "bipolar cell-like" terminal (Fig. 4B). These processes occur in addition to laterally running axons in the OPL. Polyak (1941) categorically denied that HCs in monkey retina could have descending processes to the IPL, thinking that other authors describing such cells were confusing large bipolar cells with HCs. Ramon y Cajal (1892) described inner HCs in dog and ox retinas as being "broken down into two types: HCs with descending proto-

plasmic processes and HCs without such processes." More recently, Silviera et al. (1989) have refocussed attention on the existence of "biplexiform" HCs in peripheral retinas of some mammalian species. These biplexiform HCs were revealed by neurofibrillar stains and are therefore likely to be equivalent to A-type HCs of cat (Wässle et al., 1978).

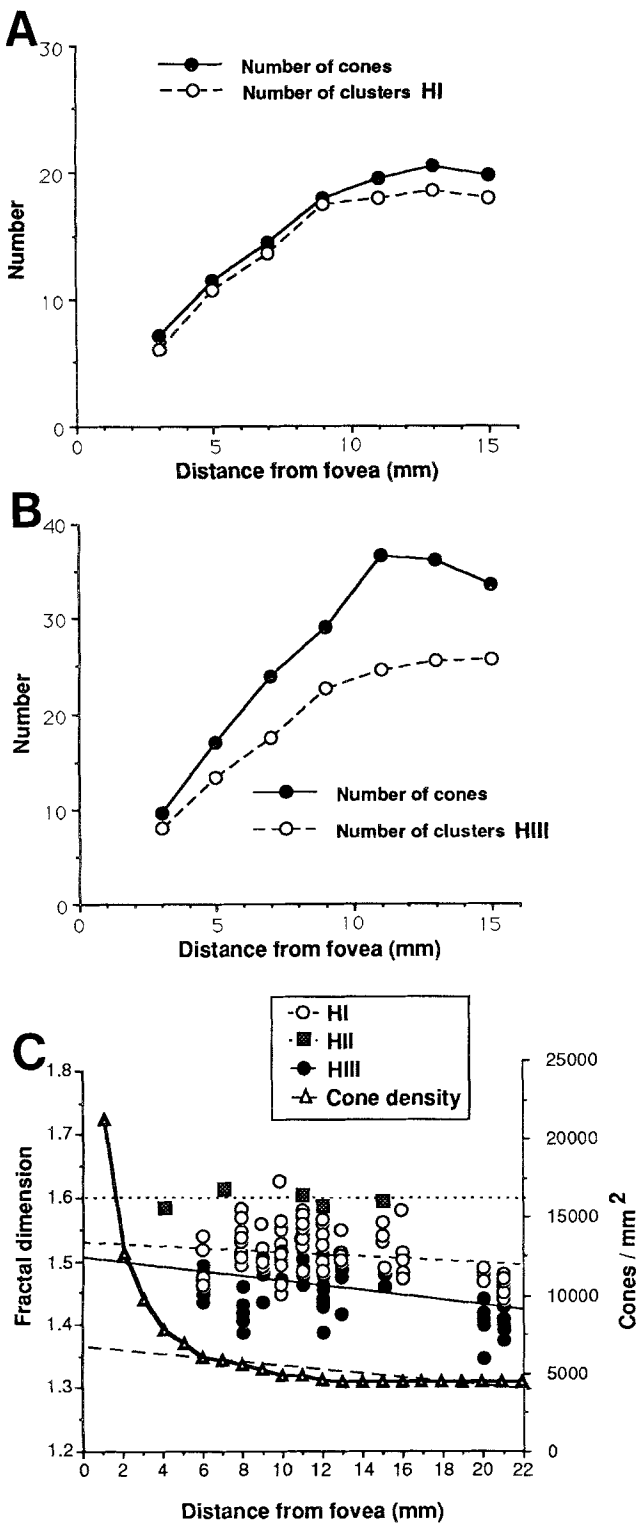

Thus, for several reasons, we now consider Cajal's inner HCs to be equivalent to A-type HCs of mammalian retinas in general (Boycott, 1974; Kolb, 1974; Mariani, 1985; Gallego, 1986). By exclusion, then, B-type HCs are considered to be equivalent to Cajal's outer HCs. What are the inner and outer HCs of Cajal's nomenclature in the human (primate) retina? HI cells, because they have an axon and morphology of the B-type cell of cat, can be considered outer HCs of Cajal. It is then possible that HII and HIII cells are the equivalents of Cajal's two types of inner HC, with HIII being the HC with the "descending protoplasmic process."

Fractal dimensions of the HCs discriminate between three different types

Knowing the fractal dimension (D value) of a neuron gives an objective measure of the profuseness of its dendritic branching and how completely the dendritic field is covered by its branches. In the case of human HCs, HII cells show the highest D value, HIII the lowest, with HI cells having an intermediate value. Another study evaluating D values of four neural classes and more than 50 different neural types in the turtle retina (Fernandez et al., 1992b, 1994) came to the conclusion that a difference in fractal value of 0.06 defined cell types. Using this criterion, then, HII cells are clearly different from HI and HIII types in the human retina. Furthermore, differences between the mean D values of 45 comparably sized cells showed that there were significant differences between HI and HII cells and HII and HIII cells ($P < 0.001$ for both). HI cells were less significantly different ($P < 0.003$) from HIII cells though, varying only by a 0.05 fractal value. Thus fractal dimensions indicate objectively what we knew subjectively, that HII cells have a much more profuse and tufted branching pattern (Kolb et al., 1980) than either HI or HIII cells, while HI and HIII cells have a similar radiate and relatively unbranched branching pattern. This might suggest that HI and HIII cells derive from a common ancestry, but HII cells have a uniquely different developmental history.

One question we asked was whether D values of HCs are related to the cone density decline with eccentricity in the human retina. As is summarized in Figure 11C,D, values of HI and HIII cells are inversely related to eccentricity and decreasing cone density. Thus both HI and HIII cells have higher D values in the foveal area of central retina than in peripheral retina. The regression lines for both classes of cell parallel the declining cone density with eccentricity (correlation of HI cells to cone density = 0.835, correlation of HIII cells to cone density = 0.836; Fig. 11C). The HII cells, on the other hand, have a flat regression line that does

Fig. 11. **A:** Graph showing the number of dendritic clusters going to cones in the dendritic fields of HI cells plotted against eccentricity. The solid line shows the number of cones expected to be present in the same area as the HI cell's dendritic fields occupy. There is a close parallel between the cluster counts (dashed line) and the expected cone counts with a 90% coincidence. **B:** Graph showing the number of dendritic clusters going to cones in HIII cells dendritic fields with eccentricity. In this case the coincidence is not as good as for the HI cells. HIII cells contact only 70% of the expected cones in their dendritic fields. **C:** D values of the three types of HC as plotted against eccentricity. At the same eccentricities, the cone counts/mm^2 from Curcio et al. (1990) are plotted. The regression lines for the HI and HIII cells are similar, with correlation coefficients of 0.835 and 0.836, respectively, to the cone distribution for a line between 4 and 22 mm from the fovea. The HII cell regression line shows no correlation to the cone distribution (−0.18).

not parallel the slope of the cone density decline at all (correlation of HII cells to cone density = −0.18; Fig. 11C). This may be another indication that HII cells have a different relationship with the cone mosaic than HI and HIII cells. The latter cells may be more related to the distributions of the G- and R-cones, which form the major components of the cone mosaic (90%) and show a decline in density with eccentricity, whereas the HII cells may be related to a different cone mosaic that maintains a relatively constant distribution density across the whole retina, i.e., the B-cone mosaic (Ahnelt et al., 1987; Curcio et al., 1990).

Why three types of HC in the human retina?

All the vertebrate animals with good color vision have cone photoreceptors whose maximal sensitivity corresponds to the three primary colors of light and an organization at the first synaptic level of cone-selective, and thus wavelength-selective, input to HCs. In these retinas, the HCs can be classified into three types both on morphological and physiological criteria (Svaetichin and MacNichol, 1958; MacNichol and Svaetichin, 1958; Spekreijse and Norton, 1970; Miller et al., 1973; Fuortes and Simon, 1974; Stell and Lightfoot, 1975; Leeper, 1978; Lipetz, 1978, 1985; Djamgoz and Downing, 1988; Kamermans et al., 1991). Models for the origin of color opponency that can be detected in second- and third-order neurons of the retina have been proposed in which a cascade of feedback and feed-forward signals occurs in the different HC types. Such models require three different HC types for creating red/green antagonism and blue/yellow antagonism. The finding of the new HIII type now adds the potential for this model to apply to trichromatic primates.

In the two accompanying papers (Ahnelt and Kolb, 1994a,b), we present evidence to support the hypothesis that the three types of HC in human retina have a color-selective bias to their cone connectivity. Thus we have been able to demonstrate that HII cells have a special connectivity pattern with the B-cones, while HIII cells avoid B-cones altogether. HI cells appear to contact all spectral cone types but with minimal involvement with the B-cones compared with the red and green cones. Although we have some distance to go before we fully understand how these different HCs might be generating color opponency at the OPL in the primate retina, the presence of the three separate units needed for the architecture of these pathways has at least now been demonstrated.

ACKNOWLEDGMENTS

We are grateful to J. Moncho for his advice on the statistical analysis. This study was supported by NIH grant EY03323 and an award from Research to Prevent Blindness (H.K., P.A.) and NIH grant EY00888 (S.K.F.). A grant from DGICYT and PM90-0111 from Spain supported E.F.

LITERATURE CITED

Ahnelt, P.K., and C. Keri (1991) Cone pedicles in the fovea and periphery of the human retina. Invest. Ophthalmol. Vis. Sci. (Suppl.) *32:*1128.

Ahnelt, P., and H. Kolb (1994a) Horizontal cells and cone photoreceptors in primate retina: A Golgi-light microscope study of spectral connectivity. J. Comp. Neurol. *343:*387–405.

Ahnelt, P., and H. Kolb (1994b) Horizontal cells and cone photoreceptors in primate retina: A Golgi-electron microscope study of spectral connectivity. J. Comp. Neurol. *343:*406–427.

Ahnelt, P.K., H. Kolb, and R. Pflug (1987) Identification of a subtype of cone photoreceptor, likely to be blue sensitive, in the human retina. J. Comp. Neurol. *255:*18–34.

Baylor, D.A., M.G.F. Fuortes, and P.M. O'Bryan (1971) Receptive fields of the cones in the retina of the turtle. J. Physiol. (London) *214:*265–294.

Boycott, B.B. (1974) Aspects of the comparative anatomy and physiology of the vertebrate retina. In R. Bellairs and E.G. Gray (eds.): Essays on the Nervous System: A Festschrift for Professor J.Z. Young. London: Oxford University Press, pp. 223–257.

Boycott, B.B., and J.E. Dowling (1969) Organization of the primate retina: Light microscopy. Phil. Trans. R. Soc. B *255:*109–184

Boycott, B.B., and H. Kolb (1973) The horizontal cells of the rhesus monkey retina. J. Comp. Neurol. *148:*115–140.

Boycott, B.B., J.M. Hopkins, and H.G. Sperling (1987) Cone connections of the horizontal cells of the rhesus monkey's retina. Proc. R. Soc. London [Biol.] *299:*345–379.

Cajal, S.R. (1892) The Structure of the Retina. Translated by S.A. Thorpe and M. Glickstein. Springfield, IL: Charles C. Thomas, 1972.

Capowski, J.J. (1989) Computer Techniques in Neuroanatomy. New York: Plenum Press.

Curcio, C.A., K.R. Sloan, R.E. Kalina, and A.E. Hendrickson (1990) Human photoreceptor topography. J. Comp. Neurol. *292:*497–523.

DeJuan, J., N. Cuenca, C, Iniguez, and E. Fernandez (1992) Axon types classified by morphometric and multivariate analysis in the rat optic nerve. Brain Res. *585:*431–434.

Djamgoz, M.B.A., and J.E.G. Downing (1988) A horizontal cell selectively contacts blue-sensitive cones in cyprinid fish retina: Intracellular staining with horseradish peroxidase. Proc. R. Soc. London [Biol.] *235:*281–287.

Dowling, J.E. (1987) The Retina: An approachable part of the brain. Cambridge, MA: The Belknap Press, Harvard University Press.

Fernandez, E., G. Guiloff, H. Kolb, J. Ammermüller, D. Zhang, and W. Eldred (1992b) Fractal dimension as a useful parameter for morphological classification of retinal neurons. Invest. Ophthalmol. Vis. Sci. Suppl. *33:*940.

Fernandez, E., W.D. Eldred, J. Ammermüller, A. Block, W. Von Bloh, and H. Kolb (1994) Complexity and scaling properties of amacrine, ganglion, horizontal and bipolar cells in the turtle retina. J. Comp. Neurol. (in press).

Fuortes, M.G.F., and E.J. Simon (1974) Interactions leading to horizontal cell responses in the turtle retina. J. Physiol. (London) *240:*177–199.

Gallego, A. (1986) Comparative studies on horizontal cells and a note on microglial cells. Progr. Ret. Res. *5:*165–206.

Gouras, P., and E. Zrenner (1981) Color vision: A review from a neurophysiological perspective. In H. Autrum, D. Ottoson, E.R. Perl, and R.F. Schmidt (eds): Progress in Sensory Physiology 1. Berlin: Springer-Verlag, pp. 139–179.

Kachigan, S.K. (1982) Cluster analysis. In: Multivariate Statistical Analysis. A Conceptual Introduction. New York: Radius, pp. 261–262.

Kamermans, M., B.W. Van Dijk, and H. Spekreijse (1991) Color opponency in cone-driven horizontal cells in carp retina. J. Gen. Physiol. *97:*819–843.

Kaneko, A. (1973) Receptive field organization of bipolar and amacrine cells in the goldfish retina. J. Physiol. (London) *213:*95–105.

Klecka, W. A. (1980) Discriminant Analysis. London: Sage.

Kolb, H. (1970) Organization of the outer plexiform layer of the primate retina: Electron microscopy of Golgi-impregnated cells. Phil. Trans. R. Soc. B *258:*261–283.

Kolb, H. (1974) The connections between horizontal cells and photoreceptors in the retina of the cat: Electron microscopy of Golgi-preparations. J. Comp. Neurol. *155:*1–14.

Kolb, H., and L.E. Lipetz (1991) The anatomical basis for colour vision in the vertebrate retina. In P. Gouras (ed): Vision and Visual Dysfunction, Vol. 6: The Perception of Colour. London: Macmillan Press, Ltd., Vol. 6, pp. 128–145.

Kolb, H., A. Mariani, and A. Gallego (1980) A second type of horizontal cell in the monkey retina. J. Comp. Neurol. *189:*31–44.

Kolb, H., K.A. Linberg, and S.K. Fisher (1992) The neurons of the human retina: A Golgi study. J. Comp. Neurol. *318:*147–187.

Leeper, H.F. (1978) Horizontal cells of the turtle retina II. Analysis of interconnections between photoreceptor cells and horizontal cells by light microscopy. J. Comp. Neurol. *182:*795–810.

Linberg, K.A., and S.K. Fisher (1988) Ultrastructural evidence that horizontal cell axon terminals are presynaptic in the human retina. J. Comp. Neurol. *268:*281–297.

Linberg, K.A., S.K. Fisher, and H. Kolb (1987) Are there three types of horizontal cell in the human retina? Invest. Ophthalmol. Vis. Sci. Suppl. *28:*262.

Lipetz, L.E. (1978) A model of function at the outer plexiform layer of cyprinid retina. In S.J. Cool and E.L. Smith (eds): Frontiers of Visual Science. Springer Series in Optical Sciences. Heidelberg: Springer-Verlag, pp. 471–482.

Lipetz, L.E. (1985) Some neuronal circuits of the turtle retina. In A. Fein and J.S. Levine (eds): The Visual System. MBL Lectures in Biology, Vol. 5. New York: Alan R. Liss, Inc., pp. 107–132.

MacNichol, E.F., and G. Svaetichin (1958) Electrical responses from isolated retina of fishes. Am. J. Ophthalmol. *42:*26–46.

Mandelbrot, B. (1982) The Fractal Geometry of Nature. New York: W.H. Freeman.

Mangel, S.C. (1991) Analysis of the horizontal cell contribution to the receptive field surround of ganglion cells in the rabbit retina. J. Physiol. (London) *442:*211–234.

Manly, B.F.J. (1986) Multivariate Statistical Methods: A Primer. London: Chapman and Hall, Ltd.

Mariani, A.P. (1985) Multiaxonal horizontal cells in the retina of the tree shrew, *Tupaia glis*. J. Comp. Neurol. *233:*553–563.

Miller, W.H., Y. Hashimoto, T. Saito, and T. Tomita (1973) Physiological and morphological identification of L- and C-type S-potentials in the turtle retina. Vision Res. *13:*443–447.

Morigiwa, K., M. Tauchi, and Y. Fukuda (1991) Fractal analysis of ganglion cell dendritic branching patterns of the rat and cat retinae. Neurosci. Res. (Suppl.) *10:*S131–S140.

Nelson, R, T. Lynn, A. Dickinson-Nelson, and H. Kolb (1985) Spectral mechanisms in cat horizontal cells. In A. Gallego and P. Gouras (eds): Neurocircuitry of the Retina: A Cajal Memorial. New York: Elsevier, pp. 109–121.

Nelson, R., R. Pflug, and S.M. Baer (1990) Background-induced flicker enhancement in cat retinal horizontal cells. II. Spatial properties. J. Neurophysiol. *64:*326–340.

Polyak, S.L. (1941) The Retina. Chicago: University of Chicago Press.

Porter, R., S. Ghosh, G.D. Lange, and T.G. Smith (1991) A fractal analysis of pyramidal neurons in mammalian motor cortex. Neurosci. Lett. *130:*112–116.

Rodieck, R.W. (1988) The primate retina. Comp. Primate Biol. (Neurosciences) *4:*203–278.

Silveira, L.C.L., E.S. Yamada, and C.W. Picanco-Diniz (1989) Displaced horizontal cells and biplexiform horizontal cells in the mammalian retina. Vis. Neurosci. *3:*483–488.

Smith, T.G., W.B. Marks, G.D. Lange, W.H. Sheriff, and E.A. Neale (1989) A fractal analysis of cell images. J. Neurosci. Methods *27:*173–180.

Spekreijse, H., and A.L. Norton (1970) The dynamic characteristics of color-coded S-potentials. J. Gen. Physiol. *56:*1–15.

Stell, W.K., and D.O. Lightfoot (1975) Color-specific interconnections of cones and horizontal cells in the retina of the goldfish. J. Comp. Neurol. *159:*473–501.

Svaetichin, G., and E.F. MacNichol Jr. (1958) Retinal mechanisms for chromatic and achromatic vision. Ann. NY Acad. Sci. *74:*385–404.

Wässle, H., and B.B. Boycott (1991) Functional architecture of the mammalian retina. Physiol. Rev. *71:*447–480.

Wässle, H., L. Peichl, and B.B. Boycott (1978) Topography of horizontal cells in the retina of the domestic cat. Proc. R. Soc. London [Biol.] *203:*269–291.

Wässle, H., B.B. Boycott, and J. Röhrenbeck (1989) Horizontal cells in the monkey retina: Cone connections and dendritic network. Eur. J. Neurosci. *1:*421–435.

Werblin, F.S., and J.E. Dowling (1969) Organization of the retina of the mudpuppy, *Necturus maculosus*. II. Intracellular recording. J. Neurophysiol. *32:*339–355.